Stem Cell Reports, Volume *18*

Supplemental Information

Organoids from mouse molar and incisor as new tools to study tooth-specific biology and development

Florian Hermans, Lara Hemeryck, Celine Bueds, Marc Torres Pereiro, Steffie Hasevoets, Hiroto Kobayashi, Diether Lambrechts, Ivo Lambrichts, Annelies Bronckaers, and Hugo Vankelecom

Supplemental Figures and Legends

Figure S1

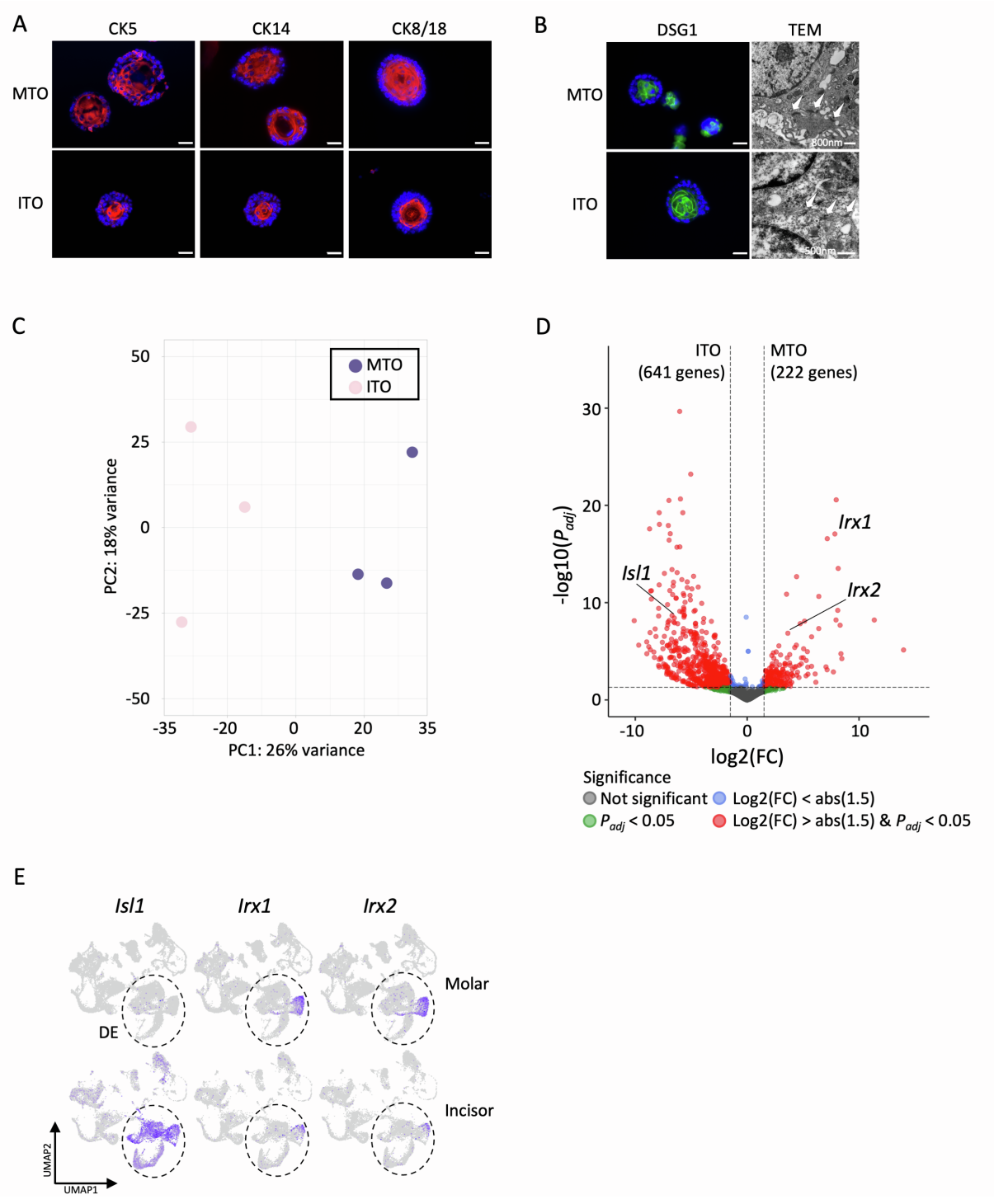

Figure S1. Additional characterization of organoids from mouse molar and incisor. Related to Figure 1. (A) IF analysis of indicated cytokeratins (CK; red) in TO. Nuclei of all IF images are counterstained with Hoechst33342. **(B)** IF (DSG1, green) and ultrastructural (TEM) characterization of desmosomes in TO. Arrows indicate desmosomes (TEM images). **(C)** PCA plot of bulk RNA-seq data from MTO and ITO (variance per component as indicated). **(D)** Volcano plot with log_2(fold change (FC)) *versus* -log10(P_{adj}) value) of RNA-seq data from MTO and ITO. Statistically upregulated genes (right for MTO and left for ITO) are indicated in red, as determined by a combination of log_2(FC) > the absolute (abs) value of ±1.5, and $P_{adj} < 0.05$. **(E)** Projection of indicated genes on our previously published mouse tooth scRNA-seq atlas (Hermans et al., 2022). The dental epithelium (DE) is circled. Scale bars: 25 μm for IF images.

Figure S2

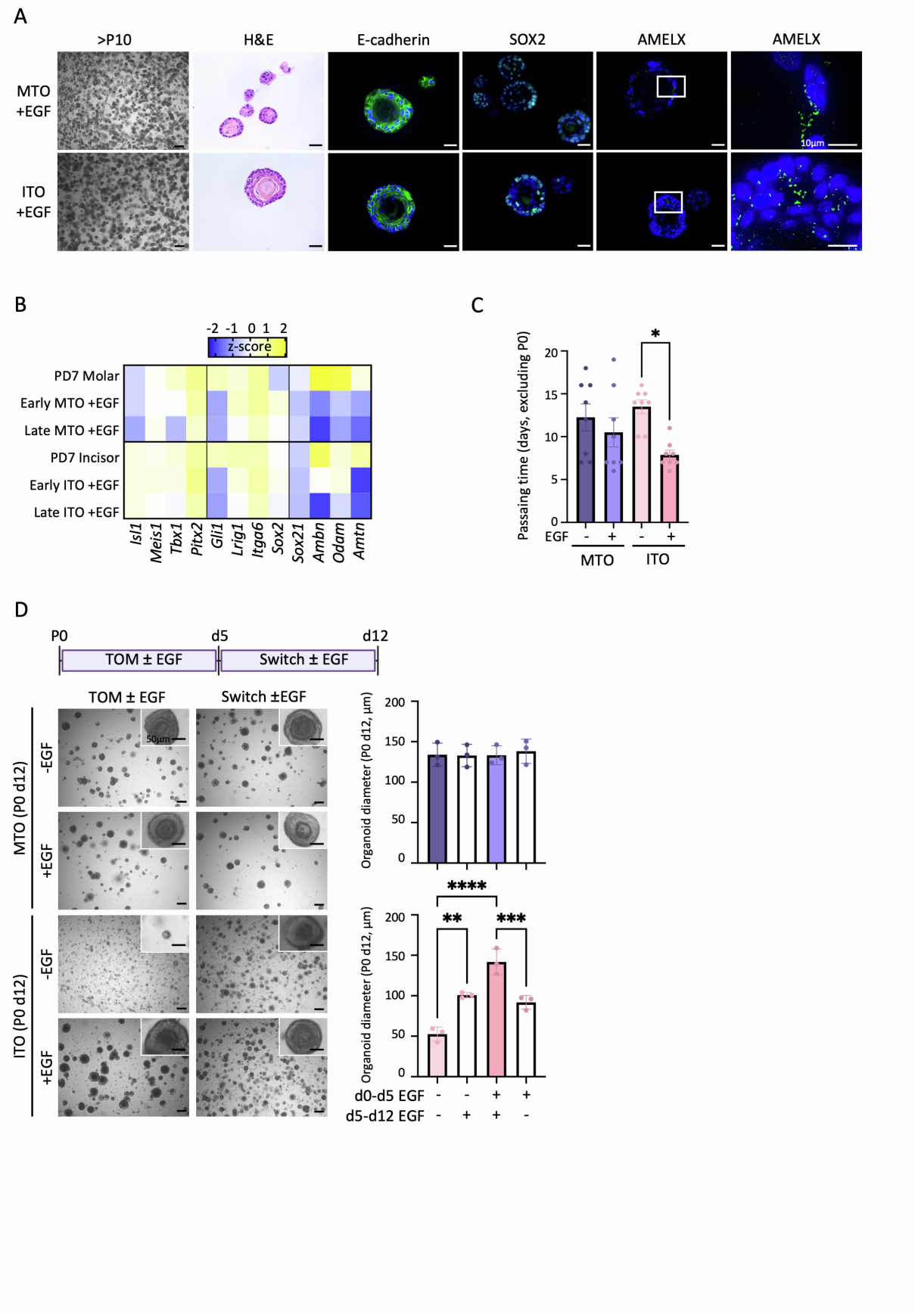
A
>P10
H&E
E-cadherin
SOX2
AMELX
AMELX
MTO +EGF
ITO +EGF
10µm
B
-2 -1 0 1 2
z-score
PD7 Molar
Early MTO +EGF
Late MTO +EGF
PD7 Incisor
Early ITO +EGF
Late ITO +EGF
Isl1
Meis1
Tbx1
Pitx2
Gli1
Lrig1
Itga6
Sox2
Sox21
Ambn
Odam
Amtn
C
Passaing time (days, excluding P0)
20
15
10
5
0
*
EGF - + - +
MTO
ITO
D
P0
d5
d12
TOM ± EGF
Switch ± EGF
TOM ± EGF
Switch ±EGF
50µm
MTO (P0 d12)
ITO (P0 d12)
-EGF
+EGF
-EGF
+EGF
Organoid diameter (P0 d12, µm)
200
150
100
50
0
****
**
***
d0-d5 EGF - - + +
d5-d12 EGF - + + -

Figure S2. Characterization of TO grown in the presence of exogenous EGF. Related to Figure 2. (A) Brightfield images of MTO and ITO grown in the presence of EGF after long-term culture for more than 10 passages (>P10); H&E and IF evaluation (of indicated markers) of organoid morphology and characteristics. Nuclei are counterstained with Hoechst33342 (blue). Boxed areas are magnified. **(B)** Heatmap of gene expression of DE TF, proposed DESC markers and EMP in primary molar and incisor tissue, early- and late-passage TO grown in the presence of EGF, as quantified by RT-qPCR analysis. Data are presented as relative expression to *Gapdh* (ΔC_t) and z-score normalized. Colors range from blue (low expression) to yellow (high expression). **(C)** Bar graph showing time between organoid passaging (days, excluding P0; mean ± SEM). Data points represent biological replicates from independently established organoid lines; one-way ANOVA with Šídák's multiple comparisons test. **(D)** *Top*: Timeline of experimental set-up. TO were seeded in P0 with or without EGF and grown for 12 days. After 5 days of initial growth in TOM with or without EGF, EGF was either removed or added from TOM ('switch'), respectively, for 7 more days. *Bottom-left***:** Brightfield images of P0 d12 organoids grown in TOM without exogenous EGF (-EGF) or with EGF (+EGF), or alternatively switched from -EGF to +EGF and *vice versa*. *Bottom-right*: Bar graphs (mean ± SEM) showing organoid diameter on d12. Data points represent biological replicates from independently established organoid lines; one-way ANOVA with Šídák's multiple comparisons test. Scale bars: 250 μm for brightfield images and 25 μm for H&E and IF images, unless indicated otherwise. **P* < 0.05, ***P* < 0.01, ****P* < 0.001, *****P* < 0.0001.

Figure S3

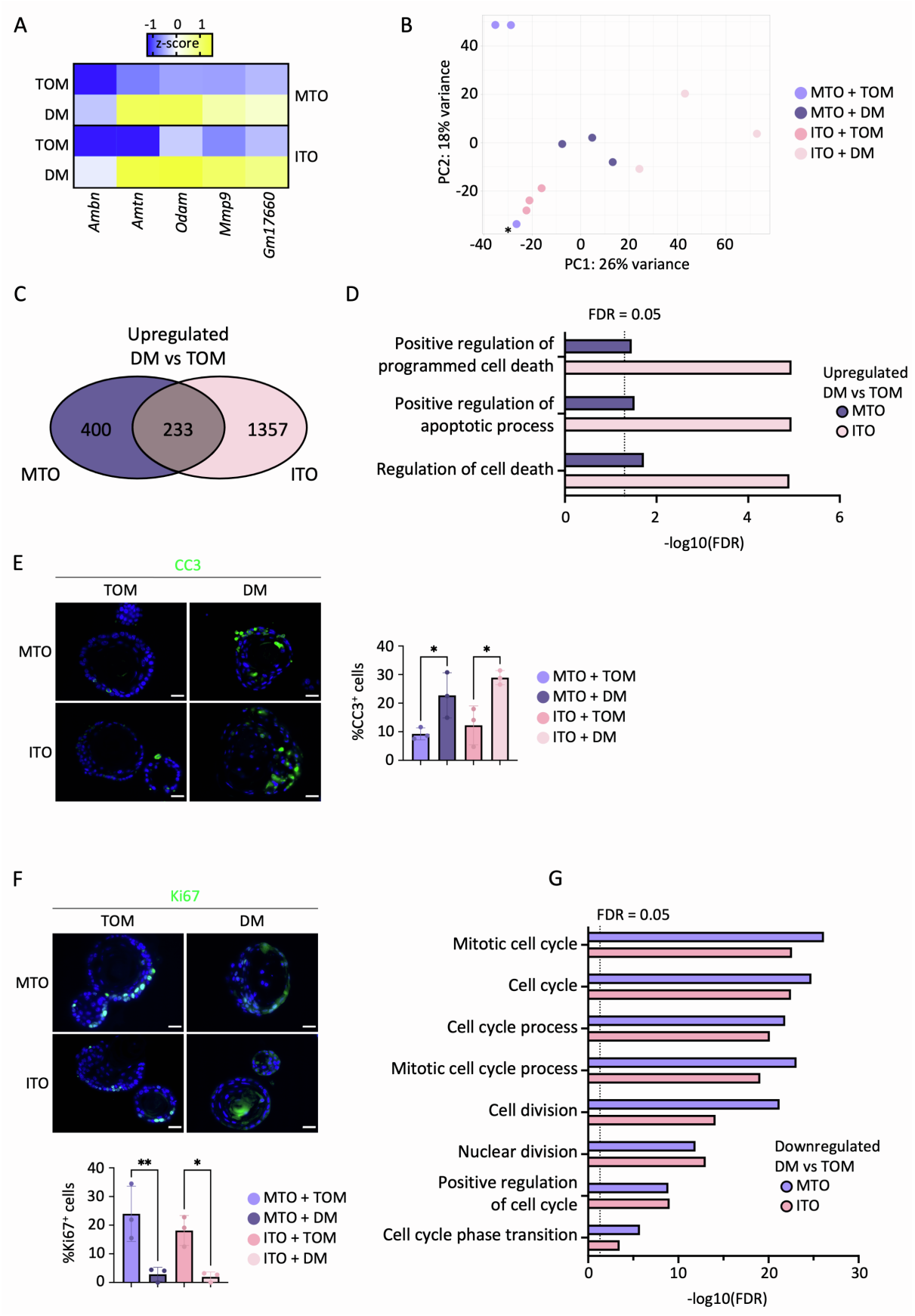
A
-1 0 1
z-score
TOM
DM
TOM
DM
MTO
ITO
Ambn
Amtn
Odam
Mmp9
Gm17660
B
PC2: 18% variance
PC1: 26% variance
MTO + TOM
MTO + DM
ITO + TOM
ITO + DM
C
Upregulated
DM vs TOM
400
233
1357
MTO
ITO
D
FDR = 0.05
Positive regulation of programmed cell death
Positive regulation of apoptotic process
Regulation of cell death
-log10(FDR)
Upregulated
DM vs TOM
MTO
ITO
E
CC3
TOM
DM
MTO
ITO
%CC3+ cells
MTO + TOM
MTO + DM
ITO + TOM
ITO + DM
F
Ki67
TOM
DM
MTO
ITO
%Ki67+ cells
MTO + TOM
MTO + DM
ITO + TOM
ITO + DM
G
FDR = 0.05
Mitotic cell cycle
Cell cycle
Cell cycle process
Mitotic cell cycle process
Cell division
Nuclear division
Positive regulation of cell cycle
Cell cycle phase transition
-log10(FDR)
Downregulated
DM vs TOM
MTO
ITO

Figure S3. *In vitro* differentiation of TO toward AB-resembling cells. Related to Figure 3. (A) Heatmap of gene expression of AB markers in TO grown in TOM or switched to DM after 7d, as quantified by RT-qPCR analysis. Data are presented as relative expression to *Gapdh* (ΔC_t) and z-score normalized. Colors range from blue (low expression) to yellow (high expression). **(B)** PCA plot of bulk RNA-seq data from TOM- and DM-grown MTO and ITO (variance per component as indicated). * indicates an outlier which was removed from subsequent analyses. **(C)** Venn diagram indicating the number of DEG upregulated in DM-*versus* TOM-grown MTO and ITO, and tooth-type overlap. **(D)** Significant (FDR ≤ 0.05, indicated by dotted line) DEG-based GO terms associated with apoptosis enriched in DM-grown TO compared to TOM-cultured controls. **(E)** *Left:* IF analysis of CC3 (green) in TO. Nuclei of all IF images are counterstained with Hoechst33342. *Right*: Bar graph (mean ± SEM) showing proportion of $CC3^+$ cells in organoids. Data points represent biological replicates from independently established organoid lines; one-way ANOVA with Šídák's multiple comparisons test. **(F)** *Top:* IF analysis of Ki67 (green) in TO. *Bottom*: Bar graph (mean ± SEM) showing proportion of $Ki67^+$ cells in organoids. Data points represent biological replicates from independently established organoid lines; one-way ANOVA with Šídák's multiple comparisons test. **(G)** Significant (FDR ≤ 0.05, indicated by dotted line) DEG-based GO terms associated with proliferation and cell cycle downregulated in DM-grown TO compared to TOM-cultured controls. Scale bars: 25 μm. *$P < 0.05$, **$P < 0.01$.

Figure S4

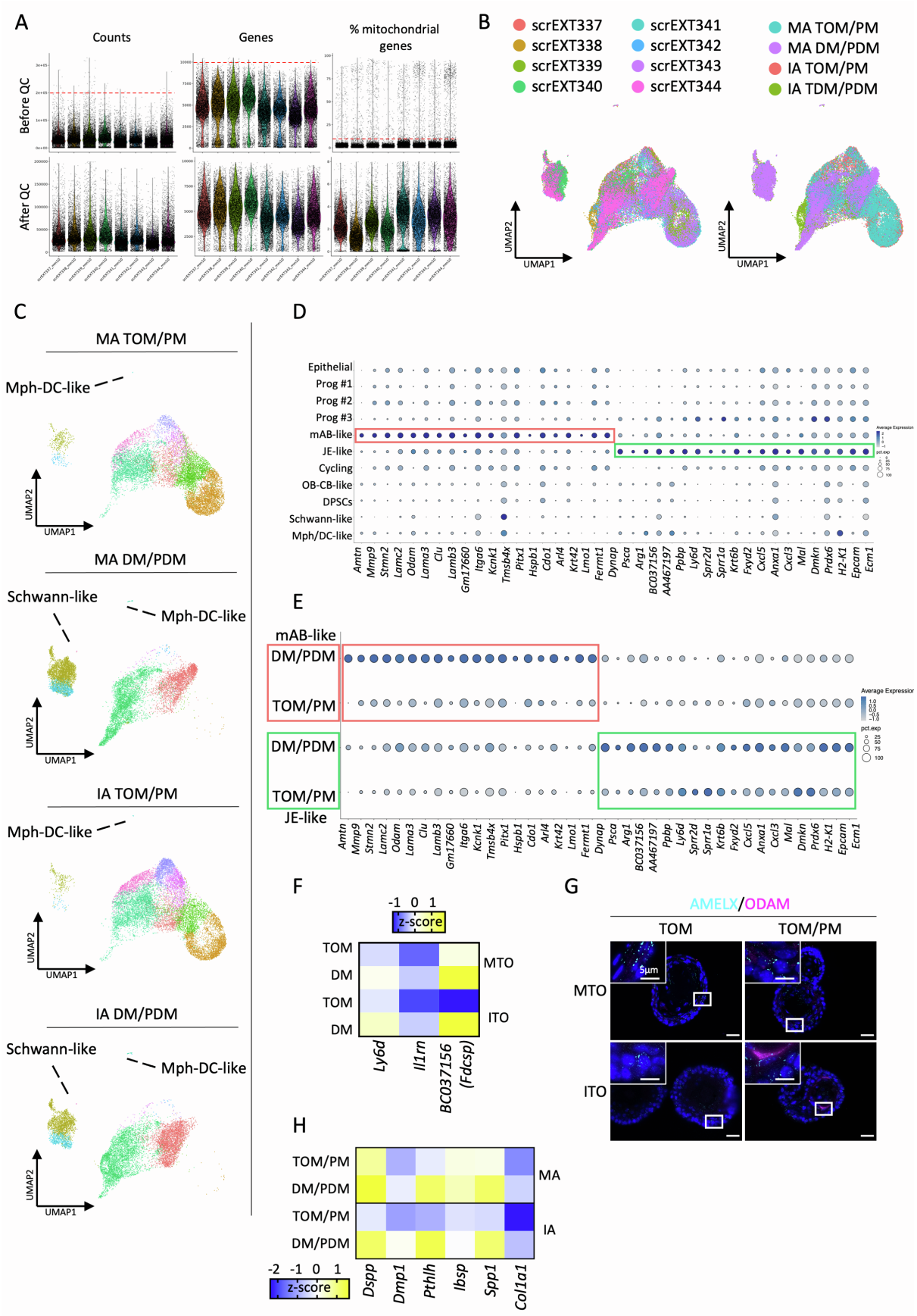
A
Counts
Genes
% mitochondrial genes
Before QC
After QC
B
scrEXT337
scrEXT338
scrEXT339
scrEXT340
scrEXT341
scrEXT342
scrEXT343
scrEXT344
MA TOM/PM
MA DM/PDM
IA TOM/PM
IA TDM/PDM
UMAP2
UMAP1
C
MA TOM/PM
Mph-DC-like
MA DM/PDM
Schwann-like
Mph-DC-like
IA TOM/PM
Mph-DC-like
IA DM/PDM
Schwann-like
Mph-DC-like
D
Epithelial
Prog #1
Prog #2
Prog #3
mAB-like
JE-like
Cycling
OB-CB-like
DPSCs
Schwann-like
Mph/DC-like
Amtn Mmp9 Stmn2 Lamc2 Odam Lama3 Clu Lamb3 Gm17660 Itga6 Kcnk1 Tmsb4x Pitx1 Hspb1 Cdo1 Arl4 Krt42 Lmo1 Fermt1 Dynap Psca Arg1 BC037156 AA467197 Ppbp Ly6d Sprr2d Sprr1a Krt6b Fxyd2 Cxcl5 Anxa1 Cxcl3 Mal Dmkn Prdx6 H2-K1 Epcam Ecm1
E
mAB-like
DM/PDM
TOM/PM
JE-like
Average Expression
pct.exp
F
z-score
TOM
DM
TOM
DM
MTO
ITO
Ly6d
Il1rn
BC037156 (Fdcsp)
G
AMELX/ODAM
TOM
TOM/PM
MTO
ITO
5μm
H
TOM/PM
DM/PDM
TOM/PM
DM/PDM
MA
IA
z-score
Dspp
Dmp1
Pthlh
Ibsp
Spp1
Col1a1

Figure S4. Quality control of tooth assembloid scRNA-seq analysis and additional characterization of developed assembloids. Related to Figure 4. (A) Violin plots showing the distribution of counts, genes and percent mitochondrial genes of the individual assembloid scRNA-seq samples before and after performing quality control (QC). Cells with values matching the following cut-offs were removed: counts >200,000, genes <1,000 and >10,000, percentage of mitochondrial genes >8%. **(B)** UMAP plots of integrated assembloid scRNA-seq data indicating individual samples (left, see Table S5) or experimental groups (right). **(C)** Annotated UMAP plots of integrated assembloid scRNA-seq datasets for MA TOM/PM- (*top*), MA DM/PDM- (*second*), IA TOM/PM- (*third*), and IA DM/PDM-grown (*bottom*) assembloids. See Figure 4C for cluster annotation. **(D)** Dotplot displaying the percentage of cells (dot size) expressing the top 20 DEG of mAB- (red box) and JE-like (green box) cells (average expression levels indicated by color intensity, see scale). **(E)** Dotplot displaying the percentage of mAB- (red) and JE-like (green) cells from TOM/PM- and DM/PDM-grown assembloids (dot size) expressing the top 20 DEG of mAB- (red box) and JE-like (green box) cells (average expression levels indicated by color intensity, see scale). **(F)** Heatmap of gene expression of JE markers in TO grown in TOM or switched to DM after 7d as quantified by RT-qPCR analysis (n=2 biological replicates from independently established organoid lines). Data are presented as relative expression to *Gapdh* (ΔC_t) and z-score normalized. Colors range from blue (low expression) to yellow (high expression). **(G)** IF analysis of AMELX (cyan) and ODAM (magenta) in TO controls grown in TOM or TOM/PM. Nuclei are counterstained with Hoechst33342 (blue). Boxed areas are magnified. **(H)** Heatmap of gene expression of markers of OB-/CB-like differentiation in tooth assembloids. Data are presented as relative expression to *Gapdh* (ΔC_t) and z-score normalized. Colors range from blue (low expression) to yellow (high expression). Scale bars: 25 μm, unless otherwise indicated.

Supplemental Tables

Table S1. Serum-free defined medium (SFDM) composition. Related to Table 1.

Product	Concentration	Supplier	Catalogue number
Sterile H_2O			
DMEM 1:1 F12 without Fe	16.8 g/L	Invitrogen	074-90715A
Bovine Serum Albumin (BSA)	5 g/L	Serva	47330.03
Catalase from bovine liver	50 μL/L	Sigma-Aldrich	C100
Ethanol absolute, ≥99.8%	600 μL/L	Fisher Chemical	E/0650DF/15
Insulin from bovine pancreas	5 mg/L	Sigma-Aldrich	I6634
$NaHCO_3$	1 g/L	Merck	106329
Penicillin	35 mg/L	Sigma-Aldrich	P3032
Streptomycin	50 mg/L	Sigma-Aldrich	S6501
Transferrin	5 mg/L	Serva	36760.01

Table S2. TO differentiation medium (DM) composition

Product	Concentration	Supplier	Catalogue number
SFDM			
B27 (without vitamin A)	2%	Gibco	12587-010
BMP2	100 ng/mL	Peprotech	120-02C
BMP4	50 ng/ML	Peprotech	120-05ET
EGF	20 ng/ML	R&D Systems	236-EG
FGF2 (=basic FGF)	20 ng/mL	R&D Systems	234-FSE
TGFβ1	4 ng/ML	R&D Systems	240-B

Table S3. Pulp medium (PM) composition

Product	Concentration	Supplier	Catalogue number
α-MEM		Sigma-Aldrich	M4526
ESGRO Recombinant LIF protein	10^3 units/mL	Sigma-Aldrich	ESG1107
Fetal Bovine Serum (FBS)	10 or 20%*	Sigma-Aldrich	F7524
FGF2 (=basic FGF)	2.5 ng/mL	R&D Systems	234-FSE
Penicillin-streptomycin	1%	Gibco	P4333

*20% FBS used for initial passage (i.e entire P0) of DPSC culture only. 10% FBS used for subsequent passages and all experiments.

Table S4. Pulp differentiation medium (PDM) composition

Product	Concentration	Supplier	Catalogue number
PM (with 10% FBS)			For composition see Table S3
Ascorbic acid	100 μM	Sigma-Aldrich	A4544
β-glycerophosphate	5 mM	Merck	35675-GM
Dexamethasone	10 μM	Sigma-Aldrich	D4902

Table S5. Metadata of assembloid scRNA-seq

Sample	Tooth derived	Condition	Medium
scrEXT337_mm10	Incisor	Control	TOM/PM
scrEXT338_mm10	Incisor	Differentiation	DM/PDM
scrEXT339_mm10	Molar	Control	TOM/PM
scrEXT340_mm10	Molar	Differentiation	DM/PDM
scrEXT341_mm10	Incisor	Control	TOM/PM
scrEXT342_mm10	Incisor	Differentiation	DM/PDM
scrEXT343_mm10	Molar	Control	TOM/PM
scrEXT344_mm10	Molar	Differentiation	DM/PDM

Table S6. Antibodies used for immunofluorescence staining

Primary antibodies

Antigen	Host	Company	Catalogue number	Dilution
AMELX	Mouse	Santa Cruz Biotechnology	365284	1:100
CC3	Rabbit	Sigma-Aldrich	AB3623	1:100
CK5	Rabbit	Biolegend	905501	1:1000
CK8/18	Guinea pig	Progen	GP11	1:200
CK14	Mouse	Thermo Fisher Scientific	MA5-11599	1:1000
DSG1	Rabbit	Proteintech	24587-1-ap	1:500
E-cadherin	Rabbit	Cell Signaling Technologies	24E10	1:400
ISL1	Rabbit	Abcam	ab20670	1:1000
Ki67	Mouse	BD Bioscience	556003	1:100
LAMC1	Rabbit	NovusBio (Biotechne)	NBP1-877118	1:200
ODAM	Rabbit	Proteintech	16509-I-AP	1:200
SOX2	Rabbit	Abcam	AB97959	1:2000
VIM	Rabbit	Cell Signaling Technologies	D21H3	1:400

Secondary antibodies

Antigen	Host	Company	Catalogue number	Dilution
Mouse IgG (A488)	Donkey	Thermo Fisher Scientific	A-21202	1:1000
Mouse IgG (A555)	Donkey	Thermo Fisher Scientific	A-31570	1:1000
Rabbit IgG (A488)	Donkey	Thermo Fisher Scientific	A-21206	1:1000
Rabbit IgG (A555)	Donkey	Thermo Fisher Scientific	A-31572	1:1000
Guinea pig IgG (FITC)	Donkey	Jackson Immunoresearch	706-096-148	1:500

Table S7. Forward and reverse primers used for qPCR gene expression analysis

Gene	Forward	Reverse
Ambn	CTGTCAACCAGGGAACCACT	TGTGATGCGGTTTAGCTGAG
Amtn	CTCAGACCGTCACATCCTCA	TGTGGATAAAGCAGGCTTCC
Areg	CCATCATCCTCGCAGCTATT	CTTGTCGAAGCCTCCTTCTT
BC037156 (Fdcsp)	AAAACTCTTCTCCTGCTCGCT	CACTGTCACTGGCACTTCGT
Btc	TTCGTGGTGGACGAGCAAACTC	CCATGACCACTATCAAGCAGACC
Col1a1	GCATGGCCAAGAAGACATCCC	GCATACCTCGGGTTTCCACG
Dmp1	CTCCTTGTGTTCCTTTGGGGG	TCTGATGACTCACTGTTCGTGG
Dspp	CAGGAACTGCAGCACAGAATGA	TATCTCACTGCCATCTGGGGA
Egf	ACTGGTGTGACACCAAGAGGTC	CCACAGGTGATCCTCAAACACG
Epgn	GAGCGAAGAAGCAGAGGTGATC	GGTCTTCCAGACAAGGATGAGAG
Ereg	CAGGCAGTTATCAGCACAACCG	CATGCAAGCAGTAGCCGTCCAT
Gapdh	ACCAGAGCATGATAAGGCAGCC	TGATGAGGCTGAAGGGTGTGAC
Gm17660	TTCCCGAATCTGTCGCTCC	TGGAACTTCCTCCGGATTGTC
Hbegf	GTCCGTCTGTCTTCTTGTCATC	CGCCCAACTTCACTTTCTCT
Ibsp	TACGGAGCAGAGACCACACC	TCTGCATCTCCAGCCTTCTTGG
Il1rn	GCTCATTGCTGGGTACTTACAA	CCAGACTTGGCACAAGACAGG
Isl1	GCTGCCTCTTTGATGGCTTCGA	CACATTCGGCACTGTTACAGCC
Itga6	CTCCTAATGCTATCTTCAAGGCG	ACCCTGAGATTGCCCAGAG
Lrig1	TTCAGCCAACGCTACCCTCACA	TAAGCCAGGTGATGCGTGGTGT
Ly6d	CAAAACCGTCACCTCAGTGGA	AGTCTGGCAGCATTGTGTGA
Meis1	GCAGTTGGCACAAGATACAGGAC	ACTGCTCGGTTGGACTGGTCTA
Mmp9	CTGGACAGCCAGACACTAAAG	CTCGCGGCAAGTCTTCAGAG
Nrg1	GCTCATCACTCCACGACTGTCA	TGCCTGCTGTTCTCTACCGATG
Nrg2	GGATGGCAAGGAACTCAACC	TCGGCCTCACAGACGTACT
Nrg3	CGAGACAAGGACCTGGCGTATT	TCACAACGGACTCCTTGGTAGC
Nrg4	TCCTCCTCACTCTTACCATCGC	GTCTCTACCAGGCTGATCTCAC
Odam	CCCTAAGATGCACAACTCGGAG	GTAGTCGGGATGCTCCTTCATG
Pitx2	CGGCAGAGGACTCATTTCAC	TTCTTGAACCAAACCCGGAC
Pthlh	GGCGTTCGGTGGAGGGGCTT	CAGATGGTGGAGGAAGAAACGG
Sox2	GAAGTGGCTGAACGAGGCATTG	TTGTCCGTGGAGGACCTTGCAT
Sox21	CCCTAAGATGCACAACTCGGAG	GTAGTCGGGATGCTCCTTCATG
Spp1	GGCAGCTCAGAGGAGAAGAAGC	AGCATTCTGTGGCGCAAGG
Tbx1	CGAGATGATCGTCACCAAGGCA	GTCATCTACGGGCACAAAGTCC

Supplemental experimental procedures

Isolation and dissociation of early-postnatal mouse molar and incisor tissue

C57BL/6 PD7 mice (pool of male and female) were used for tooth isolation, obtained by breeding in the Animal Housing Facility of the KU Leuven under conditions of constant temperature, humidity, 12-hour light-dark cycle and *ad libitum* access to food and water. Experiments were approved by the KU Leuven Ethical Committee for Animal Experimentation (P056/2022).

Pups were euthanized by decapitation, after which the mandibles were collected in Dulbecco's Modified Eagle Medium with 10 mM HEPES (DMEM; Gibco), supplemented with 10% fetal bovine serum (FBS; Sigma-Aldrich) and 1% penicillin-streptomycin (Gibco). Whole (unerupted) molars, including surrounding dental follicle and attached epithelium, as well as apical ends of (unerupted) incisors were carefully isolated, rinsed with phosphate-buffered saline (PBS; Gibco) and incubated with 2.5% Trypsin (Gibco) for 30 minutes at 37°C. Following trypsinization, the dental follicle and attached epithelium were manually recovered from the molars, and the dental pulp was separately collected from the molar pulp chamber. Subsequently, the molar (either dental follicle and attached epithelium or collected dental pulp tissue) and incisor tissues were further enzymatically digested with TrypLE Express (Gibco) supplemented with 5 µM ROCK inhibitor (ROCKi, Y-27632; Thermo Fisher) for 15 minutes at 37°C, and mechanically triturated (using syringes with decreasing diameters: 18G (Terumo), 20G (BD) and 26G (BD)) to a suspension containing single cells and small cell clusters. The number of collected cells was determined with a Z2 Coulter Particle Count and Size analyzer using COULTER Z2 AccuComp software (Beckman Coulter).

Establishment and passaging of mouse TO

The dissociated molar and incisor DE cell material was resuspended in serum-free defined medium (SFDM; Thermo Fisher Scientific; Table S1) and growth factor-reduced Matrigel (Corning) at a 30:70 ratio, supplemented with 10 µM ROCKi. Cells were seeded at 20,000 and 12,500 cells per 20 µL drop from molars and incisors, respectively. After solidification, pre-warmed TOM (Table 1) was added. Organoid cultures were kept at 37 °C in a 1.9% CO_2 incubator (as required by the SFDM buffering system), and medium was refreshed every 2 days. To passage the TO as occurring every 7-10 days, Matrigel droplets were collected using ice-cold SFDM, followed by incubation with TrypLE containing 5 µM ROCKi and mechanical trituration to dissociate the organoids. Remaining (large) organoid fragments were allowed to sediment, and the cell number in the supernatant, containing single cells and small fragments, was determined as described above. Upon reaching stable growth, dissociated MTO and ITO were seeded at 15,000-20,000 cells and 7,500 cells per 20 µL droplet, respectively. Organoids could be cryopreserved to be stored in liquid nitrogen, and be brought again in culture after thawing, all as previously described (Boretto et al., 2017; Cox et al., 2019).

To inhibit EGFR signaling, TO were treated with AG-1478 (1 µg/mL; Sigma-Aldrich) or EKI-785 (1 µM; Selleckchem) for 12 days from initial DE cell seeding. To explore TO differentiation capacity, organoids from passage 5 (P5) were grown in TOM for 7 days, and subsequently switched to culture in DM (Table S2) for 7 days. The DM was optimized by removing multiple growth factors from TOM one by one, and subsequently adding BMP2, BMP4 and TGFβ1. As initial readout for DM optimization, gene expression of EMP was assessed (*Ambn*, *Amtn*, *Odam*). Brightfield pictures of organoids were recorded using an Axiovert 40 CFL microscope (Zeiss).

DPSC culture

DPSC were obtained and cultured as previously described (Collignon et al., 2019). Briefly, molar pulp cells were seeded onto 0.1% gelatin-coated plates (gelatin from porcine skin; Sigma-Aldrich) and cultured in PM with 20% FBS (Table S3). Upon reaching 70-80% confluency, cells were dissociated using TrypLE and replated in PM with 10% FBS. The obtained DPSC were passaged every 7-10 days.

Establishment of mouse tooth assembloids

Tooth assembloids were established using a similar protocol as we previously described for human tooth assembloids (Hemeryck et al., 2022). Briefly, after dissociating TO (from P2-P3) and DPSC (from P2-P3), both matched and derived in the same tooth isolation experiment, into single cells as described above, both cell types were combined in round-bottom low-attachment plates (96-well; Greiner). Using a layered approach, 5,000 DPSC were first seeded by sedimentation (300 g for 1 min at 4 °C), followed by 5,000 MTO- or ITO-derived cells sedimented on top (300 g for 1 min at 4 °C) (Nakao et al., 2007). The cell composite was provided with 10% growth-factor reduced Matrigel and 90% of either a 1:1 mixture of TOM/PM or DM/PDM (Tables 1, S2-4). After 24 h incubation at 37 °C and 5% CO_2, the formed structures were collected and plated in 20 µL droplets of 70% Matrigel to generate tooth

assembloids which were maintained in the respective 1:1 media mixtures at 37 °C and 5% CO_2. Brightfield pictures of assembloids were recorded using an Axiovert 40 CFL microscope (Zeiss).

Histochemical and immunostaining analysis
Organoids were fixed in paraformaldehyde (PFA, 4% in PBS; Merck) for 30 min at room temperature (RT) and subsequently paraffin-embedded with an Excelsior ES Tissue Processor (Thermo Fisher Scientific). Paraffin sections of 5 µm thickness were obtained with a Microm HM 30 microtome (Thermo Fisher Scientific) and subjected to hematoxylin and eosin (H&E) or immunofluorescence (IF) staining. For IF analysis, antigen retrieval with citrate buffer (pH6; at 95°C) and permeabilization (0.1% Triton X-100; Sigma-Aldrich) were performed. For detection of ISL1, antigen retrieval was done with Tris-EDTA (pH9; at 95°C). Next, blocking buffer (0.15% glycine (VWR), 2 mg/mL BSA (Serva), 0.1% Triton-X in PBS) with 10% donkey serum (Sigma-Aldrich) was added for 1 h at RT. After incubation with primary antibodies and subsequently secondary antibodies (Table S6), and nuclei counterstaining with Hoechst33342 (1:1000; Merck), sections were mounted with ProLong Gold Antifade Mountant (Thermor Fisher Scientific). Images were recorded using a Leica DM5500 upright epifluorescence microscope (Leica Microsystems) accessible through the Imaging Core (VIB, KU Leuven), and analyzed and converted to pictures with Fiji imaging software. For visualization of $AMELX^+$ signals, the Fiji 'subtract background' function was used with a rolling ball radius of 3 pixels. Representative images are shown.

EdU labelling of TO
EdU labelling in TO was performed using the Click-iT EdU Alexa Fluor 488 kit (Thermo Fisher Scientific) according to the manufacturer's instructions, involving the incubation of organoids with EdU (10 µM) for 2 h. Images were recorded on a Zeiss LSM 780 – SP Mai Tai HP DS (Cell and Tissue Imaging Cluster (CIC), KU Leuven), and analyzed and converted to pictures with Fiji imaging software. Representative images are shown.

TEM analysis
Organoid samples were prepared for TEM as previously described in detail (Lambrichts et al., 1993; Cox et al., 2019). Samples were fixed in 2.5% glutaraldehyde (Sigma-Aldrich), dehydrated, embedded in epoxy resin, and cut into 40-70 nm sections. TEM images were acquired with the JEM1400 transmission electron microscope (JEOL) equipped with an Olympus SIS Quesmesa 11 Mpxl camera, or the Philips EM208 S electron microscope (Philips) equipped with the Morada Soft Imaging System camera with corresponding iTEM-FEI software (Olympus SIS), or a JEOL-1400 FLASH (JEOL) with Xarosa camera (EMSIS).

Gene expression analysis by qPCR
Total RNA was extracted from dissociated molar and incisor tissue, TO and tooth assembloids using the GenElute Mammalian Total RNA Miniprep kit (Sigma-Aldrich) following manufacturer's instructions. RNA was reverse-transcribed (RT) using the Superscript III First-Strand Synthesis Supermix kit (Thermo Fisher Scientific). The resultant cDNA samples were analyzed with SYBR Green-based quantitative (q)PCR with the Platinum SYBR Green qPCR SuperMix-UDG kit (Invitrogen) and using specific forward and reverse primers (Table S7), as described before (Cox et al., 2019). Glyceraldehyde-3-phosphate dehydrogenase (*Gapdh)* was included as housekeeping gene. Gene expression levels were calculated as ΔCt values relative to *Gapdh* ($Ct_{target} - Ct_{housekeeping}$). Z-score normalization was performed by subtracting the mean ΔCt of the experiment and dividing by the standard deviation of the obtained ΔCt values for each measurement.

Bulk RNA-seq analysis
RNA was isolated from P0 MTO and ITO grown in TOM (n=3 biological replicates per condition), or from P5 MTO and ITO grown in TOM+EGF and exposed to DM or not (n=3 biological replicates per condition). Total RNA was isolated using the GenElute Mammalian Total RNA Miniprep kit (Sigma-Aldrich) following manufacturer's instructions, and RNA Integrity Number (RIN) determined with Agilent Picochips on an Agilent BioAnalyzer 2100 (Agilent Technologies). Samples with RIN > 7.5 were sequenced (Nucleomics Core, VIB/KU Leuven). TruSeq total stranded RNA library preparation was performed, followed by sequencing on a NovaSeq 6000 instrument (Illumina). Data are accessible from ArrayExpress database (accession number E-MTAB-12557). Following quality control, reads were aligned to the mouse reference genome (*Mus musculus*, GRCm38/mm10 release M21) and transcript abundancies were quantified using Salmon (1.4.0) (Patro et al., 2017). Gene-level count matrices were created using the tximport package (v1.18.0) and used as input for DEG analysis with DESeq2 (v1.30.1) as previously reported (Love et al., 2014; Soneson et al., 2016). PCA analysis was performed using the

plotPCA function from the DESeq2 package after rlog transformation. Based on PCA analysis, one MTO+TOM sample was considered an outlier and omitted from further downstream analyses. For visualization and gene ranking, log fold change (LFC) estimates were shrunk using the apeglm (v1.12.0) method for effect size shrinkage as described (Love et al., 2014; Zhu et al., 2019). Volcano plots were generated using the EnhancedVolcano package (v1.6.0) (https://github.com/kevinblighe/EnhancedVolcano). GO analysis (FDR < 0.05) of DEG ($log_2FC > 1.5$ and *P*adj < 0.05) was executed with the GO webplatform (www.geneontology.org) (Ashburner et al., 2000; Carbon et al., 2021). Enriched pathway values are presented as $-log_{10}$(FDR).

scRNA-seq analysis

MA and IA, exposed to DM or not (2 replicates per condition), were dissociated into single cells using 0.25% Trypsin (Gibco; supplemented with 5μM ROCKi) treatment and mechanical trituration, collected in 0.04% BSA (in PBS) and filtered through a Flowmi 40 μm cell strainer (Sigma-Aldrich). Single cells were loaded onto 10X Genomics cartridge according to the manufacturer's instructions. Generation of barcoded libraries was performed with the Chromium Single-cell 3' v2 Chemistry Library Kit, Gel Bead & Multiplex Kit and Chip Kit (10× Genomics). The libraries were sequenced on an Illumina NextSeq and NovaSeq6000. Data are accessible from ArrayExpress database (accession number E-MTAB-12544). Raw sequencing reads were demultiplexed, mapped to the mouse reference genome (mm10) and gene expression matrices were generated using CellRanger (v5.0.0; 10× Genomics).

Downstream analysis was performed in Seurat (v4.0.0) as previously described (Stuart et al., 2019; Hao et al., 2021; Hermans et al., 2022). Briefly, low quality cells and potential doublets were removed based on the number of counts (>200,000) and genes (<1,000 and >10,000) per cell, as well as the percentage of mitochondrial genes (>8%) expressed per cell. After quality control, data were normalized and variable features identified (using the NormalizeData and FindVariableFeatures functions), and the data were integrated by the combination of tooth type and medium condition (i.e. MA+TOM/PM, MA+DM/PDM, IA+TOM/PM and IA+DM/PDM) using the FindIntegrationAnchors (with default parameters and dims = 1:30) and the IntegrateData functions. After scaling of expression levels, integrated data were subjected to PCA. Uniform Manifold Approximation and Projection (UMAP) dimensionality reduction was performed (with umap.method=uwot, using the top 50 PC and with min.dist=0.5). Initial clustering and annotation were performed, prior to correction of count matrices for ambient/background RNA using the SoupX (v1.5.0) package (Young and Behjati, 2020). The global contamination fractions were estimated to be 1.7%, well within normal range (0–10%).

Using the SoupX corrected counts, data were integrated using the reciprocal PCA (rPCA) method (Hao et al., 2021). Therefore, after data normalization and identification of variable features, each individual dataset was scaled and subjected to PCA analysis, which was used as input to the FindIntegrationAnchors function (with dims=1:30 and reduction='rpca') after which the datasets were integrated across all features using the IntegrateData function. During the scaling of the data, cell cycle regression was performed. Lists of human S and G2M genes were obtained from Seurat and converted to their mouse orthologues as input for the CellCycleScoring function. Following integration, the dataset was subjected to PCA, after which the top 50 PC were used for UMAP dimensionality reduction (with umap.method=uwot and min.dist=0.5) and clustering. Clustering and annotation were finalized using resolution 1.2 and 50 (to allow separation of the Schwann-like cluster) and evaluation of marker expression. DEG analysis between AB-like and JE-like clusters was performed in Seurat with the SoupX-corrected counts using the FindMarkers function with logfc.threshold=0.5 and min.pct=0.5.

Subcutaneous transplantation of ITO

Matrigel with d7 ITO (P5) was pipetted into custom-made 3D-printed hydroxyapatite scaffolds (Sirris) which were s.c. transplanted in immunodeficient nu/nu mice (Janvier Labs), as in detail described elsewhere (Bronckaers et al., 2021; Hemeryck et al., 2022). Scaffolds with only Matrigel were used as negative controls. One week later, implants were resected, and grafts carefully extracted and fixed in 4% PFA before processing for H&E or IF staining as described above. This study was approved by the Ethical Committee on Animal Experiments (ECAE) of UHasselt (protocol 202138).

Chicken CAM assay

Fertilized chicken eggs (*gallus gallus*) were incubated for 3 days at 37 °C and constant humidity. Next, 3 ml of albumen was removed and eggs were again incubated until embryonic day (E) 9 as previously in detail described (Bronckaers et al., 2013). Subsequently, pre-solidified 30 µl Matrigel droplets with d7 ITO (P5) were applied onto the CAM following the creation of a 1 cm^2 window into the shell to expose the CAM. Droplets of Matrigel alone served as negative controls. The window was covered with

cellophane tape and eggs were returned to the incubator. One week later, the CAM was removed and fixed in 4% PFA for H&E and IF analysis (described above).

Statistical analysis

Statistical analyses were performed using GraphPad Prism (v9.3.1) for macOS and are specified in the figure legends. All experiments were performed with ≥ 3 independent biological replicates (i.e. organoid lines established from independent mouse litters) unless otherwise indicated.

Supplemental references

Ashburner, M., Ball, C. A., Blake, J. A., Botstein, D., Butler, H., Cherry, J. M., et al. (2000). Gene Ontology: tool for the unification of biology. *Nat Genet* 25, 25–29. doi: 10.1038/75556.

Boretto, M., Cox, B., Noben, M., Hendriks, N., Fassbender, A., Roose, H., et al. (2017). Development of organoids from mouse and human endometrium showing endometrial epithelium physiology and long-term expandability. *Development* 144, 1775–1786. doi: 10.1242/dev.148478.

Bronckaers, A., Hilkens, P., Fanton, Y., Struys, T., Gervois, P., Politis, C., et al. (2013). Angiogenic Properties of Human Dental Pulp Stem Cells. *PLoS One* 8, e71104. doi: 10.1371/journal.pone.0071104.

Bronckaers, A., Hilkens, P., Wolfs, E., and Lambrichts, I. (2021). "By the Skin of Your Teeth: A Subcutaneous Mouse Model to Study Pulp Regeneration," in *Vascular Morphogenesis. Methods in Molecular Biology*, ed. D. Ribatti (Humana Press Inc.), 223–232. doi: 10.1007/978-1-0716-0916-3_16.

Carbon, S., Douglass, E., Good, B. M., Unni, D. R., Harris, N. L., Mungall, C. J., et al. (2021). The Gene Ontology resource: enriching a GOld mine. *Nucleic Acids Res* 49, D325–D334. doi: 10.1093/nar/gkaa1113.

Collignon, A. M., Castillo-Dali, G., Gomez, E., Guilbert, T., Lesieur, J., Nicoletti, A., et al. (2019). Mouse Wnt1-CRE-RosaTomato Dental Pulp Stem Cells Directly Contribute to the Calvarial Bone Regeneration Process. *Stem Cells* 37, 701–711. doi: 10.1002/stem.2973.

Cox, B., Laporte, E., Vennekens, A., Kobayashi, H., Nys, C., Van Zundert, I., et al. (2019). Organoids from pituitary as a novel research model toward pituitary stem cell exploration. *Journal of Endocrinology* 240, 287–308. doi: 10.1530/JOE-18-0462.

Hao, Y., Hao, S., Andersen-Nissen, E., Mauck, W. M., Zheng, S., Butler, A., et al. (2021). Integrated analysis of multimodal single-cell data. *Cell* 184, 3573-3587.e29. doi: 10.1016/j.cell.2021.04.048.

Hemeryck, L., Hermans, F., Chappell, J., Kobayashi, H., Lambrechts, D., Lambrichts, I., et al. (2022). Organoids from human tooth showing epithelial stemness phenotype and differentiation potential. *Cellular and Molecular Life Sciences* 79, 153. doi: 10.1007/s00018-022-04183-8.

Hermans, F., Bueds, C., Hemeryck, L., Lambrichts, I., Bronckaers, A., and Vankelecom, H. (2022). Establishment of inclusive single-cell transcriptome atlases from mouse and human tooth as powerful resource for dental research. *Front Cell Dev Biol* 10, 1021459. doi: 10.3389/fcell.2022.1021459.

Lambrichts, I., Creemers, J., and Van Steenberghe, D. (1993). Periodontal neural endings intimately relate to epithelial rests of Malassez in humans. A light and electron microscope study. *J Anat* 182, 153.

Love, M. I., Huber, W., and Anders, S. (2014). Moderated estimation of fold change and dispersion for RNA-seq data with DESeq2. *Genome Biol* 15, 550. doi: 10.1186/s13059-014-0550-8.

Nakao, K., Morita, R., Saji, Y., Ishida, K., Tomita, Y., Ogawa, M., et al. (2007). The development of a bioengineered organ germ method. *Nat Methods* 4, 227–230. doi: 10.1038/nmeth1012.

Patro, R., Duggal, G., Love, M. I., Irizarry, R. A., and Kingsford, C. (2017). Salmon provides fast and bias-aware quantification of transcript expression. *Nat Methods* 14, 417–419. doi: 10.1038/nmeth.4197.

Soneson, C., Love, M. I., and Robinson, M. D. (2016). Differential analyses for RNA-seq: transcript-level estimates improve gene-level inferences. *F1000Res* 4, 1521. doi: 10.12688/f1000research.7563.2.

Stuart, T., Butler, A., Hoffman, P., Hafemeister, C., Papalexi, E., Mauck, W. M., et al. (2019). Comprehensive Integration of Single-Cell Data. *Cell* 177, 1888-1902.e21. doi: 10.1016/j.cell.2019.05.031.

Young, M. D., and Behjati, S. (2020). SoupX removes ambient RNA contamination from droplet-based single-cell RNA sequencing data. *Gigascience* 9, giaa151. doi: 10.1093/gigascience/giaa151.

Zhu, A., Ibrahim, J. G., and Love, M. I. (2019). Heavy-tailed prior distributions for sequence count data: removing the noise and preserving large differences. *Bioinformatics* 35, 2084–2092. doi: 10.1093/bioinformatics/bty895.